The Astrophysical Journal, 661: L85–L88, 2007 May 20


# DISCOVERY OF EXTREME ASYMMETRY IN THE DEBRIS DISK SURROUNDING HD 15115

Paul Kalas,[1,2] Michael P. Fitzgerald,[1,2] and James R. Graham[1,2]
*Received 2006 December 18; accepted 2007 April 4; published 2007 May 3*

## ABSTRACT

We report the first scattered light detection of a dusty debris disk surrounding the F2 V star HD 15115 using the *Hubble Space Telescope* in the optical and Keck adaptive optics in the near-infrared. The most remarkable property of the HD 15115 disk relative to other debris disks is its extreme length asymmetry. The east side of the disk is detected to ∼315 AU radius, whereas the west side of the disk has radius >550 AU. We find a blue optical to near-infrared scattered light color relative to the star that indicates grain scattering properties similar to the AU Mic debris disk. The existence of a large debris disk surrounding HD 15115 adds further evidence for membership in the $\beta$ Pic moving group, which was previously argued based on kinematics alone. Here we hypothesize that the extreme disk asymmetry is due to dynamical perturbations from HIP 12545, an M star east of HD 15115 that shares a common proper motion vector, heliocentric distance, galactic space velocity, and age.

*Subject headings:* circumstellar matter — stars: individual (HD 15115)

## 1. INTRODUCTION

Volume-limited, far-infrared surveys of the solar neighborhood suggest that ∼15% of main-sequence stars have excess thermal emission indicative of circumstellar grains (Aumann 1985; Backman & Paresce 1993; Meyer et al. 2007). Direct imaging of dust-scattered light reveals the geometry of the grain population relative to the star, which further elucidates the origin of dust. In some cases, a circumstellar nebulosity may be amorphous with asymmetric striated features produced when stellar radiation pressure deflects interstellar dust (Kalas et al. 2002). In other cases, such as $\beta$ Pic and Fomalhaut, the geometry of dust is consistent with a circumstellar disk or belt related to the formation of planetesimals (Smith & Terrile 1984; Kalas et al. 2005). Although larger bodies such as comets and asteroids are not directly observed, they most likely exist as a reservoir for injecting fresh debris into the system over the lifetime of the star. Furthermore, circumstellar debris disks display significant structure and asymmetry that may be linked, in principle, to dynamical perturbations from a planetary system (Roques et al. 1994; Liou & Zook 1999; Moro-Martín & Malhotra 2002). Unfortunately, only ∼10% of stars with excess thermal emission have detected scattered light disks due to the high contrast between the host star and the low surface brightness nebulosity at optical and near-infrared wavelengths. Fortunately, the observational capabilities have improved in recent years due to instrument upgrades on the *Hubble Space Telescope* (*HST*) and the implementation of adaptive optics (AO) on large, ground-based telescopes.

Here we show new scattered light images of a debris disk surrounding HD 15115, an F2 star at 45 pc (Table 1), first reported as a source of thermal excess emission by Silverstone (2000). The spectral energy distribution is consistent with a single temperature dust belt at ∼35 AU radius with an estimated dust mass of 0.047 $M_\oplus$ (Zuckerman & Song 2004; Williams & Andrews 2006). Recently, Moór et al. (2006) identified HD 15115 as a candidate for membership in the 12 Myr old $\beta$ Pic moving group (BPMG), based on new radial velocity measurements that resulted in galactic kinematics similar to those of the BPMG.

## 2. OBSERVATIONS AND DATA ANALYSIS

We first detected the HD 15115 disk in scattered light using the *HST* ACS High Resolution Channel (HRC) on 2006 July 17. We use the F606W broadband filter and the 1.8″ diameter occulting spot to artificially eclipse the star. Three flat-fielded frames of 700 s each from standard pipeline processing of the *HST* data archive were median-combined for cosmic-ray rejection. The point-spread function (PSF) was then subtracted iteratively using five other stars of similar spectral type obtained from the *HST* archive. The relative intensity scaling between images was iteratively adjusted until the residual image showed a mean radial profile equal to zero intensity perpendicular to the circumstellar disk. The images were then corrected for geometric distortion, resulting in a 25 mas pixel$^{-1}$ scale.

The resulting optical images revealed a needle-like feature projecting westward from the star to the edge of the field, but with almost no counterpart to the east. Given the high degree of asymmetry that could conceivably arise from instrumental scattering, we endeavored to confirm the disk using the Keck II telescope with AO on 2006 October 7 and 2007 January 26. Using the near-infrared camera NIRC2, a 0.4″ radius occulting spot and a 10 mas pixel scale, we confirmed the existence of the disk in $J$ (1.2 $\mu$m), $H$ (1.6 $\mu$m), and $K'$ (2.2 $\mu$m). PSF subtraction is accomplished by allowing the sky to rotate relative to the detector, thereby separating the stellar PSF from the disk. The observing procedure and data reduction procedure are fully described in Fitzgerald et al. (2007). Due to poor observing conditions in October, including intermittent cirrus clouds, we used only the best fraction of data by visually selecting frames of relatively constant intensity and PSF sharpness. The resulting effective integration times are 450, 980, and 600 s for $J$, $H$, and $K'$, respectively. Standard star observations were obtained under similar, nonphotometric conditions and processed in a similar manner. In 2007 January we reobserved HD 15115 (1930 s cumulative integration time) and two standard stars under photometric conditions from Keck using the same instrumentation with the $H$ broadband filter. However, the observations were made after meridian transit and the limited rotation of the sky relative to the instrumental PSF causes disk emission to be included in the PSF estimate,

[1] Astronomy Department and Radio Astronomy Laboratory, University of California, Berkeley, CA 94720.

[2] National Science Foundation Center for Adaptive Optics, University of California, Santa Cruz, CA 95064.

TABLE 1
STELLAR PROPERTIES

| Parameter | HD 15115 | HIP 12545 | Reference |
|---|---|---|---|
| Spectral type ...... | F2 | M0 | *Hipparcos* |
| $m_V$ (mag) .......... | 6.79 | 10.28 | *Hipparcos* |
| Mass ($M_\odot$) ........ | 1.6 | 0.5 | Cox (2006) |
| Distance (pc) ...... | $44.78^{+2.22}_{-2.01}$ | $40.54^{+4.38}_{-3.61}$ | *Hipparcos* |
| R.A. (ICRS) ....... | 02 26 16.2447 | 02 41 25.89 | *Hipparcos* |
| Decl. (ICRS) ...... | +06 17 33.188 | +05 59 18.41 | *Hipparcos* |
| $\mu_\alpha$(mas yr$^{-1}$) ....... | 86.09 ± 1.09 | 82.32 ± 4.46 | *Hipparcos* |
| $\mu_\delta$ (mas yr$^{-1}$) ...... | −50.13 ± 0.71 | −55.13 ± 2.45 | *Hipparcos* |
| $\mu_\alpha$(mas yr$^{-1}$) ....... | 87.1 ± 1.2 | 82.3 ± 4.3 | Tycho-2 |
| $\mu_\delta$ (mas yr$^{-1}$) ...... | −50.9 ± 1.2 | −55.1 ± 2.7 | Tycho-2 |
| $U$ (km s$^{-1}$) ........ | −13.2 ± 1.9 | −14.0 ± 0.5 | ...[a] |
| $V$ (km s$^{-1}$) ......... | −17.8 ± 1.2 | −16.7 ± 0.9 | ...[a] |
| $W$ (km s$^{-1}$) ........ | −6.0 ± 2.3 | −10.0 ± 0.5 | ...[a] |

[a] Galactic kinematics for HD 15115 and HIP 12545 from Moór et al. (2006) and Song et al. (2003), respectively.

resulting in disk self-subtraction at small radii. Our analysis of the 2007 January data therefore yields a detection of the west ansa in the region 1.3″–3.3″ radius. The photometry in this second epoch agrees well with that of the first epoch (on average, the 2007 January disk photometry is 0.13 mag arcsec$^{-2}$ fainter than 2006 October), suggesting that our frame selection technique for the first epoch of cloudy conditions effectively filtered out nonphotometric data.

## 3. RESULTS

Figure 1 shows the PSF-subtracted images of HD 15115 with *HST* and with Keck. The west side of the disk in the optical *HST* data has P.A. = 278°.5 ± 0.5 and is detected from the edge of the occulting spot at 1.5″ (67 AU) radius to the edge of the field at 12.38″ (554 AU) radius. The east midplane is detected as far as ~7″ (315 AU) radius. At this radius the east midplane begins to intersect the outer portion of the coronagraph's 3.0″ occulting spot. Further east, past the spot and to the edge of the field, no nebulosity is detected 9.0″–14.9″ radius. The appearance of the disk is more symmetric in the 2006 October Keck data, which show the disk between 0.7″ (31 AU) and 2.5″ (112 AU).

Optical surface brightness contours (Fig. 2) reveal a sharp midplane morphology for the west extension that indicates an edge-on orientation to the line of sight. The west midplane is qualitatively similar to that of $\beta$ Pic's northeast midplane, including a characteristic width asymmetry (Kalas & Jewitt 1995; Golimowski et al. 2006). The northern side of the west midplane is more vertically extended than the southern side. For example, the full width at half-maximum across the disk midplane at 2″ radius is 0.19″ ± 0.10″ in both the optical and NIR data. However, the vertical cuts are not symmetric about the midplane when measuring the half-width at quarter-maximum (HWQM). The HWQM north of the west midplane is 1.6 ± 0.1 times greater than that of the HWQM south of the west midplane. This width asymmetry is confirmed in the Keck data. If the width asymmetry is found to be in the opposite direction in the opposite midplane, then Kalas & Jewitt (1995) refer to such a feature as the butterfly asymmetry. The butterfly asymmetry is evident in the morphology of $\beta$ Pic that Golimowski et al. (2006) recently related to the presence of a second disk midplane tilted relative to the main disk midplane. However, our detection of HD 15115's east midplane has insufficient signal-to-noise to confirm the presence of a width asymmetry here.

We note that none of the surface brightness profiles show evidence for significant flattening inward toward the star (Fig. 3). All four surface brightness profiles are well represented by a single power-law decrease with radius. If there is an inner dust depletion, then it resides within a 40 AU radius. This constraint is consistent with model fits of the spectral energy distribution that place the dominant emitting dust component at ~35 AU radius (Zuckerman & Song 2004; Williams & Andrews 2006).

The color of the disk may be estimated in the 2.0″–3.3″ region where the *H*-band and *V*-band data overlap (Fig. 3). At

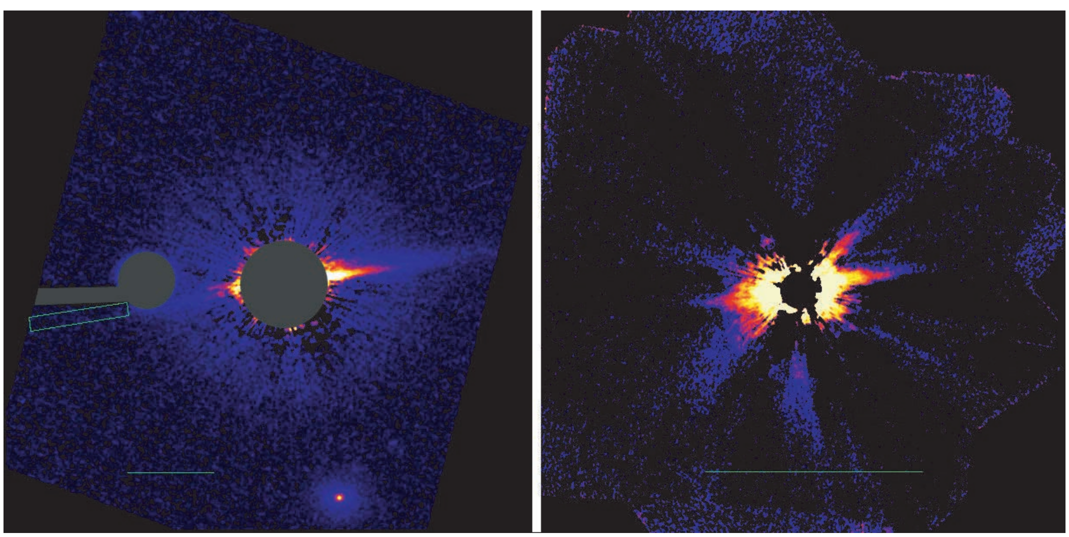

FIG. 1.—False-color, log scale images of the HD 15115 disk as originally discovered using the ACS/HRC F606W ($\lambda_c$ = 591 nm, $\Delta\lambda$ = 234 nm; *left*) and confirmed in *H* band with Keck II adaptive optics (*right*; 2006 October 26 data). North is up, east is left, and the scale bars span 5″. In the *HST* image we use gray fields over the occulting bar and a 3.0″ occulting spot located to the left of HD 15115, as well as a gray disk covering PSF-subtraction artifacts surrounding HD 15115 itself. If the HD 15115 disk were a symmetric structure, then the east side of the disk would have been detected within the rectangular box, shown below the ACS/HRC occulting finger. The NIR data (*right*) show a more symmetric disk within a 2″ radius, with asymmetry becoming more apparent beyond the 2″ radius. Due to poor observing conditions, the field is contaminated by residual noise due to the diffraction pattern of the telescope (e.g., at 2 o'clock and 7 o'clock relative to HD 15115). However, whereas the residual diffraction pattern noise of the telescope rotates relative to the sky orientation over a series of exposures, the image of the disk remains fixed and it is confirmed as real.

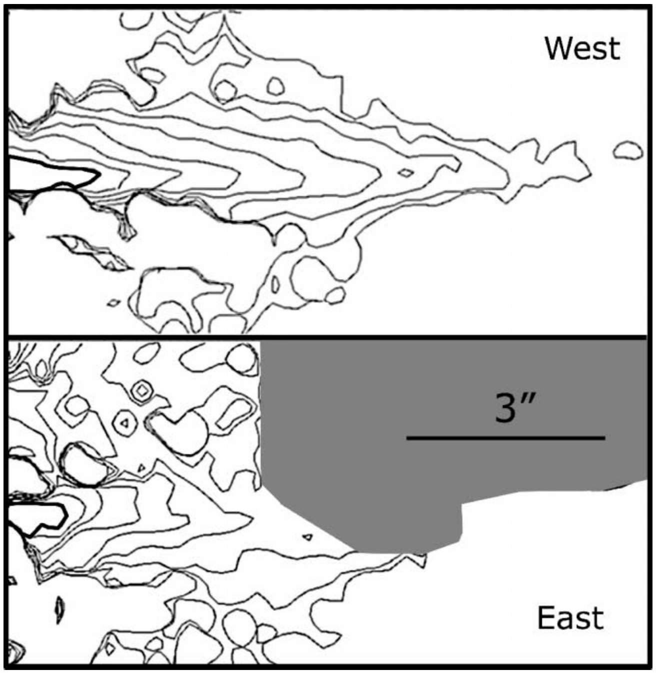


FIG. 2.—Surface brightness isocontours for the HD 15115 debris disk converted from F606W to Johnson *V* band (derived using STSDAS/SYNPHOT with a Kurucz model atmosphere and the appropriate observatory parameters). The disk was rotate by 8° clockwise such that the midplane lies along a horizontal line. The bottom frame is the east extension, transposed across the vertical axis, and the gray region marks the area occupied by the ACS/HRC occulting finger and 3.0″ occulting spot. The left edge of the frame corresponds to a 2″ radius from the star. The innermost contour (*bold*) is 19.0 mag arcsec$^{-2}$, and the outermost contour represents 23.0 mag arcsec$^{-2}$, with a contour interval of 0.5 mag arcsec$^{-2}$.

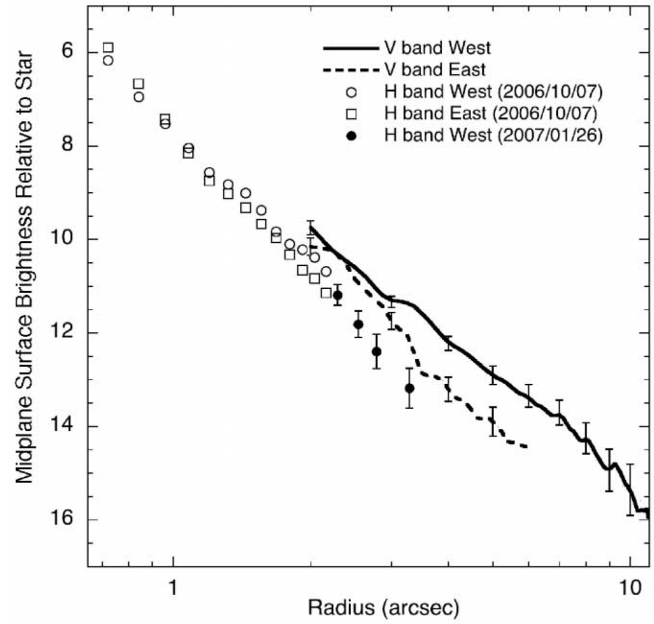


FIG. 3.—Radial surface brightness (mag arcsec$^{-2}$) distribution along the west and east midplanes of HD 15115. We plot the difference between the measured disk surface brightness and the stellar magnitudes of $H = 5.86$ and $V = 6.80$. Disk photometry was extracted from boxes 0.25″ × 0.25″ centered on the midplane. We plot a representative sample of error bars that gives the standard deviation of the background residuals as a function of radius. The aperture corrections derived from point source photometry are 0.48 and 0.57 for the *H*-band data in the 2006 October and 2007 January observations, respectively, and 0.70 for the *V*-band data. The *H*-band radial profiles between 0.7″ and 2.3″ radius may be described by power laws with indices −3.7 and −4.4 for the west and east disk extensions, respectively. In the *V* band, the east midplane profile can be fit by a power law with index −4.0 between 2.0″ and 6.0″ radius. Thus, our data do not show a significant color gradient as a function of radius for the east ansa. The west midplane profile in the *V* band can be fit by a single power law with index −3.0 between 2.0″ and 10.0″ radius. This profile is significantly shallower than the *H*-band profile, resulting in a blue color gradient as a function of radius for the west ansa.

face value, $\Sigma_V - \Sigma_H \approx -0.6$ mag arcsec$^{-2}$ at 2″ radius, increasing to −1.9 mag arcsec$^{-2}$ at 3.3″ radius for the West disk extension. The east ansa has similar blue scattering at 2″ radius, but the *V*-band surface brightness profile is steeper in the east than in the west, giving a roughly constant blue color with increasing radius in the east.

In a future paper we will present a detailed model of dust scattering and thermal emission properties, which requires a more complicated treatment of the obvious disk asymmetry. However, for isotropically scattering grains in an edge-on disk, an analytic approach shows that the grain number density distribution as a function of radius within the disk midplane follows a power law with index equivalent to 1 minus the sky-projected radial midplane power-law index. From the Keck data in Figure 3, we estimate that the disk number density distribution decreases with disk radius as $r^{-3}$ in the inner region up to ∼3.3″ radius for both sides of the disk. At >3.3″ radius, the optical data show that this profile continues for the east extension, but that the disk number density profiles flattens for the west extension, as described in Figure 3. A precise measurement of the color and polarization of the disk-scattered light is necessary to further constrain the grain size distribution, the corresponding scattering phase function and albedo, and the effect on the disk number density profile.

## 4. DISCUSSION

Asymmetric disk structure is evident in the majority of debris disks, and most authors invoke planetary perturbations as the likely origin. Secular perturbations may offset the center of global disk symmetry from the location of the star, although this effect may also be produced by an external perturber (Wyatt et al. 1999). The edge-on debris disk surrounding $\beta$ Pic displays a variety of radial and vertical asymmetries on large scales (Kalas & Jewitt 1995) that may be most relevant to the study of HD 15115. In the deepest optical images of the $\beta$ Pic disk, the northeast and southwest disk midplanes are traced to 1835 and 1450 AU, respectively, giving a ratio of 1.27 (Larwood & Kalas 2001). In the case of HD 15115 the corresponding ratio is >1.75. This ratio is a lower limit given that the 550 AU extent of the west midplane is limited only by our field of view.

A single stellar flyby, or a periodic flyby by a bound companion on an eccentric orbit, has been studied as a potential mechanism for producing $\beta$ Pic's large-scale asymmetry (Larwood & Kalas 2001). However, in a kinematic study of *Hipparcos*-detected stars with published radial velocities, Kalas et al. (2001) did not find any perturbers that approached closer than 0.6 pc of $\beta$ Pic, although the sample was estimated as only 20% complete. In the case of HD 15115, Moór et al. (2006) noted that another $\beta$ Pic moving group member, HIP 12545, is located relatively nearby in sky position.

Table 1 summarizes the observed properties of both stars. Their projected separation is 3.9°, which translates to 2.9 pc at a mean heliocentric distance of 43 pc. Within the uncertainties, the proper motion vectors, the (*U*, *V*) galactic space motions, and heliocentric distance are identical. Furthermore, the eastward location of HIP

12545 is in the direction of the truncated side of the HD 15115 debris disk. This geometry is consistent with the dynamical simulation of a disk disrupted by a stellar flyby in Larwood & Kalas (2001). Specifically, in their Figure 18, the long end of a highly perturbed disk is located in the direction of periastron. The perturber follows a parabolic trajectory such that in a later epoch it is located in the direction opposite of periastron, or in the direction of the truncated side of the disk. Periastron in these models is ∼700 AU, with an initial disk radius of ∼500 AU. Overall, the ensemble of evidence favors further consideration of HD 15115 and HIP 12545 as a possible wide-separation multiple system with a highly eccentric orbit ($e > 0.95$).

A prediction of the Larwood & Kalas (2001) model is that the perturber may capture disk material and display a tenuous and highly asymmetric tail of escaping material pointing away from the mother disk. To test the hypothesis that HD 15115 suffered a close encounter with HIP 12545, high-contrast observations of HIP 12545 should reveal circumstellar nebulosity due to captured material. Since this is captured material, the nebulosity may not resemble a disk, and any tail should point away from the mother disk (eastward).

To futher investigate this hypothesis, we examined ACS/HRC coronagraphic observations of HIP 12545 obtained by program GO-10487 (PI: David Ardila). The observing technique is similar to that described here for HD 15115. After PSF subtraction, we do not detect nebulosity in the vicinity of HIP 12545. Therefore, the possibility that the extreme disk asymmetry of HD 15115 is created by dynamical interactions with HIP 12545 does not have further supporting evidence at the present time.

Finally, we note that among the four debris disks imaged in scattered light in the BPMG, the dust appears depleted for HD 15115. The values of dust optical depth in $10^{-4}$ units are given as 24.3 ± 1.1, 4.9 ± 0.4, 29.3 ± 1.6, and 4.0 ± 0.3 for $\beta$ Pic (A5 V), HD 15115 (F2 V), HD 181327 (F5.5 V) and AU Mic (M2 V), respectively (Moór et al. 2006). The factor of ∼5 smaller optical depth for HD 15115 compared to $\beta$ Pic and HD 181327 suggests a different evolutionary path for the disk. Although a stellar flyby is one possibility, migration and dynamical instabilities within a hypothetical planetary system may also play a role in the rapid diminution of dust parent bodies around HD 15115 (e.g., Morbidelli & Valsecchi 1997).

## 5. SUMMARY

Optical and near-infrared coronagraphic images of the F2 star HD 15115 reveal a highly asymmetric debris disk with an edge-on orientation. We describe the morphological and photometric properties of the disk, deferring a detailed model of scattering and thermal emission of grains to future work. The blue scattered light color may indicate grain properties most similar to those of the AU Mic debris disk, where $\Sigma_V - \Sigma_H \approx -1$ mag arcsec$^{-2}$ relative to the star (Fitzgerald et al. 2007), and less like those of $\beta$ Pic, which is predominantly red scattering (Golimowski et al. 2006). A key follow-up measurement would be polarization, which in the case of AU Mic revealed highly porous macroscopic grains (Graham et al. 2007).

With outer optical radius >550 AU, HD 15115 possesses the second largest debris disk next to $\beta$ Pic. However, the length asymmetry between its west and east midplanes greatly exceeds that of $\beta$ Pic and other disks. HD 15115 is now the fourth debris disk discovered in scattered light among the $\beta$ Pic moving group members. Future work should test our hypothesis that extreme asymmetries are due to dynamical perturbations from the nearby M star HIP 12545.

Support for GO-10896 was provided by NASA through a grant from STScI under NASA contract NAS5-26555.

## REFERENCES

Aumann, H. H. 1985, PASP, 97, 885
Backman, D. E., & Paresce, F. 1993, in Protostars and Planets III, ed. E. H. Levy & J. I. Lunine (Tucson: Univ. Arizona Press), 1253
Cox, A., ed. 2006, Allen’s Astrophysical Quantities (New York: Springer)
Fitzgerald, M. P., Kalas, P., Duchene, G., Pinte, C., & Graham, J. R. 2007, ApJ, submitted
Golimowski, D. A., et al. 2006, AJ, 131, 3109
Graham, J. R., Kalas, P., & Matthews, B. 2007, ApJ, 654, 595
Kalas, P., Deltorn, J.-M., & Larwood, J. 2001, ApJ, 533, 410
Kalas, P., Graham, J. R., Beckwith, S. V. W., Jewitt, D. C., & Lloyd, J. P. 2002, ApJ, 567, 999
Kalas, P., Graham. J. R., & Clampin, M. C. 2005, Nature, 435, 1067
Kalas, P., & Jewitt, D. 1995, AJ,110, 794
Larwood, J. D., & Kalas, P. 2001, MNRAS, 323, 402
Liou, J.-C., & Zook, H. A. 1999, AJ, 118, 580
Meyer, M. R., Backman, D. E., Weinberger, A. J., & Wyatt, M. C. 2007, in Protostars and Planets V, ed. B. Reipurth, D. Jewitt, & K. Keil (Tucson: Univ. Arizona Press), 573
Moór, A., Abraham, P., Derekas, A., Kiss, C., Kiss, L. L., Apai, D., Grady, C., & Henning, T. 2006, ApJ, 644, 525
Morbidelli, A., & Valsecchi, G. B. 1997, Icarus, 128, 464
Moro-Martín, A., & Malhotra, R. 2002, AJ, 124, 2305
Roques, F., Scholl, H., Sicardy, B., & Smith, B. A. 1994, Icarus, 108, 37
Silverstone, M. D., 2000 Ph.D. thesis, Univ. California, Los Angeles
Smith, B. A., & Terrile, R. J. 1984, Science, 226, 1421
Song, I., Zuckerman, B., & Bessel, M. S. 2003, ApJ, 599, 342
Williams, J. P., & Andrews, S. M. 2006, ApJ, 653, 1480
Wyatt, M. C., Dermott, S. F., Telesco, C. M., Fisher, R. S., Grogan, K., Holmes, E. K., & Piña, R. K. 1999, ApJ, 527, 918
Zuckerman, B., & Song, I. 2004, ApJ, 603, 738